Biophysical Chemistry 137 (2008) 126–132

Contents lists available at ScienceDirect

Biophysical Chemistry

journal homepage: http://www.elsevier.com/locate/biophyschem

Role of electrostatics on membrane binding, aggregation and destabilization induced by NAD(P)H dehydrogenases. Implication in membrane fusion

César L. Avila [a], Beatriz F. de Arcuri [a], Fernando Gonzalez-Nilo [b], Javier De Las Rivas [c], Rosana Chehín [a,*], Roberto Morero [a]

[a] Departamento Bioquímica de la Nutrición, Instituto Superior de Investigaciones Biológicas (CONICET-UNT) and Instituto de Química Biológica Dr. Bernabé Bloj, Chacabuco 461 (4000), Tucumán, Argentina
[b] Centro de Bioinformática y Simulación Molecular, Universidad de Talca, Avenida Lircay s/n, 3460000, Talca, Chile
[c] Grupo de Bioinformática y Genómica Functional, Instituto de Biología Molecular y Celular del Cáncer (IBMCC-CIC, CSIC/USAL) Campus Miguel de Unamuno s/n. Salamanca, Spain

ARTICLE INFO

Article history:
Received 12 July 2008
Received in revised form 8 August 2008
Accepted 8 August 2008
Available online 23 August 2008

Keywords:
Protein–membrane interactions
Membrane fusion
FDPB

ABSTRACT

Glyceraldehyde-3-phosphate dehydrogenase (GAPDH) is considered a classical glycolytic protein that can promote the fusion of phospholipid vesicles and can also play a vital role on *in vivo* fusogenic events. However, it is not clear how this redox enzyme, which lack conserved structural or sequence motifs related to membrane fusion, catalyze this process. In order to detect if this ability is present in other NAD(P)H dehydrogenases with available structure, spectroscopic studies were performed to evaluate the capability of alcohol dehydrogenase (ADH), glutamic dehydrogenase (GDH) and sorbitol dehydrogenase (SDH) to bind, aggregate, destabilize and fuse vesicles. Based on finite difference Poisson–Boltzmann calculations (FDPB) the protein–membrane interactions were analyzed. A model for the protein–membrane complex in its minimum free energy of interaction was obtained for each protein and the amino acids involved in the binding processes were suggested. A previously undescribed relationship between membrane destabilization and crevices with high electropositive potential on the protein surface was proposed. The putative implication of the non-specific electrostatics on NAD(P)H dehydrogenases induced membrane fusion is discussed.

1. Introduction

Phospholipid bilayers form the barriers that define and partition all living cells and thus, membrane remodeling through fusion and fission is crucial in numerous intra and intercellular events such as: membrane trafficking, myotube formation, secretory exocytosis, fertilization and virus infection. Phospholipid membranes do not fuse spontaneously since the process is energetically unfavorable because biological membranes are subjected to strong repulsive hydration electrostatic and steric barriers [1]. These barriers can be overcome mainly by the presence of different agents such as divalent cations and/or proteins.

Protein-mediated membrane fusion was extensively studied and the best characterized systems are those involved in the enveloped virus infection [2] and membrane trafficking [3]. The biophysics of membrane fusion is dominated by the stalk hypothesis. According to this view, fusion of pure lipid membranes requires at least five distinct steps: approach to small distances; local perturbation of the lipid structure and merger of proximal monolayers; stalk formation; stalk expansion, which in some variants of the stalk model is associated with a hemi fusion diaphragm; and, finally, pore formation [4].

Structural and functional analyses have revealed similarities between viral and intracellular fusion where a four helical bundle folding leads to the apposition of two membranes and provides the energy for the fusion reaction [4].

During viral infection, the protein interaction with the target membrane involves an hydrophobic stretch of about 15 residues called "the fusion peptide" [5]. This segment was initially identified either at the N-terminus, as in most orthomyxoviruses, paramyxoviruses and several retroviruses [5,6]; or in the interior of the fusion proteins, as in *Rous sarcoma* virus [7], Vesicular Stomatitis virus [8], or Ebola virus [9]. It was generally accepted that each viral fusion protein contains a single fusion peptide and this segment was the sole responsible for the destabilization of the target cell membrane. However, new evidences indicate that in addition to classical fusion peptides, other regions from viral fusion

Abbreviations: GAPDH, glyceraldehyde-3-phosphate dehydrogenase; GDH, glutamic dehydrogenase; SDH, sorbitol dehydrogenase; ADH, alcohol dehydrogenase; DOPC, dioleyl phosphatidylcholine; DOPS, dioleyl phosphatidylserine; SUV, small unilamellar vesicles; DPA, dipicolinic acid; EDTA, ethylenediaminetetraacetic acid; ANTS, 8-aminonaphthalene-l,3,6-trisulfonic acid; DPX, *p*-xylene-bispyridinium bromide; HMM, hidden Markov Model; PDB, protein data bank; NBD-PE, N-(7-nitro-2,1,3-benzoxadiazol-4-yl)-phosphatidylethanolamine; Rh-PE, N-(lissamine rhodamine B sulfonyl)-phosphatidylethanolamine.

* Corresponding author. Tel./fax: +54 381 4248921.
E-mail address: rosana@fbqf.unt.edu.ar (R. Chehín).

0301-4622/$ – see front matter © 2008 Elsevier B.V. All rights reserved.
doi:10.1016/j.bpc.2008.08.003

proteins interact with membranes, contributing to their merging. Nevertheless, the precise function for each region is still unclear [10].

In addition to the viral and SNARE proteins, GAPDH is a cytoplasmic redox protein that can also promote the fusion of phospholipid vesicles [11,12]. Moreover, several independent studies demonstrated that GAPDH also plays a vital role on *in vivo* fusogenic events [13].

In the present work, the study is extended over some other NAD(P)H dehydrogenases with structural data available. In this way, spectroscopic studies were performed to evaluate the capability of ADH, GAPDH, GDH and SDH to bind, aggregate, destabilize and fuse vesicles. Based on computational tools, along with the availability of structural data, a model that could explain the molecular basis of these phenomena was constructed. Using FDPB calculations, the most probable orientation of each protein in relation to the membrane was obtained and the putative amino acids involved in the binding process were proposed. The two-dimensional representation of the binding free energy as a function of the protein rotation angles provides information about its vesicle aggregation capability. The protein–membrane complex obtained also suggested that these enzymes expose to the membrane a concave surface with high electropositive potential which could be related to the bilayer destabilization.

2. Materials and methods

2.1. Chemicals

Bovine liver glutamic dehydrogenase (EC 1.4.1.3), rabbit muscle glyceraldehyde-3-phosphate dehydrogenase (EC 1.2.1.12), baker's yeast alcohol dehydrogenase (EC 1.1.1.1), sheep liver sorbitol dehydrogenase (EC 1.1.1.14) from Sigma Chem. Co, were dissolved in 20 mM Tris–HCl buffer pH 7.4 and used immediately. DOPC and DOPS were obtained from Avanti Polar lipids. NBD-PE and Rh-PE were purchased from Molecular Probes Inc.

2.2. Vesicle preparation

DOPC with appropriate amount of DOPS was dissolved in chloroform:methanol (2:1, v/v) and dried under nitrogen onto the wall of a Corex glass tube and then placed in a vacuum oven to completely remove any remaining solvent. The lipid was then rehydrated in 20 mM Tris–HCl buffer pH 7.4, and the large multilamellar vesicles formed were sonicated on ice under nitrogen with probe-type sonifier. Cycles of sonication (1-min pulse) and cooling (1 min) were repeated up to 20 times until the initially cloudy lipid dispersion became clear. In order to obtain small unilamellar vesicle (SUV) suspension free of titanium particles, the suspension was centrifuged for 15 min at 1100 ×g [14].

2.3. Protein–membrane binding assays

The accessibility of the protein Trp to aqueous quenchers was studied by monitoring the changes in the Trp fluorescence emission spectra upon addition of SUV [15]. Corrected spectra were obtained by subtracting the light scattering of SUV alone. The quenching experiments were carried out by the addition of KI on a 0.1 μM protein solution in the absence or presence of 50 μM SUVs. The lipid–protein mixtures (molar ratio of 500:1) were incubated for 1 h at room temperature prior to the measurements. The quenching constants were obtained from the slope of the Stern–Volmer plots of F_0/F vs. [KI], where F_0 and F are the fluorescence intensities in the absence and presence of quencher, respectively [16]. The slope of the Stern–Volmer plot, obtained from the quenching experiments, is the Stern–Volmer constant (K_{SV}). This parameter (K_{SV}) is related to the exposure degree (accessibility) of Trp residues to the water soluble quencher. In general, when the slope increases a high degree of exposure is implied, assuming that there is not a large difference in fluorescence lifetime.

2.4. Aggregation measurements

Liposome aggregation was estimated as an increase in light scattering after protein addition, measured in an ISS spectrofluorometer with both monochromators set at 450 nm. The protein:lipid molar ratio used was the same as for the protein–membrane binding assays.

2.5. Leakage measurements

The release of the liposomal content was measured by following the fluorescence quenching of pre-encapsulated Tb/DPA complex upon release into the external medium containing 0.1 mM EDTA [17]. To prepare vesicles containing Tb–DPA complex trapped within, the dried lipid film was resuspended in the appropriated buffer (20 mM Tris–HCl pH 7.40) containing a 1:1 mixture of 15 mM $TbCl_3$ and 150 mM DPA (sodium salt). After sonication, non-encapsulated material was removed by molecular sieve chromatography on Sephadex G-75. Excitation and emission wavelengths were 278 and 545 nm respectively, while a high-pass cutoff filter (>490 nm, a 3–71 filter, Corning, Corning, NY) was placed before the emission monochromator to minimize contributions from light scattering. The fluorescence scale was calibrated so that 0% and 100% leakage corresponded to the Tb/DPA fluorescence intensities in the original vesicles and in the presence of 0.2 % Triton X_{100}, respectively. The measurements were done in an ISS spectrofluorometer.

2.6. Fusion measurements

Lipid mixing assays were performed following a modification of the method of Struck et al. [18]. Two liposomes population were prepared with either 1.0 mol% of NBD-PE (donor) or 2.0 mol% of Rh-PE (acceptor). Lipid mixing between both populations resulted in a decrease of the relative N-NBD-PE fluorescence due to resonance energy transfer between the two probes. The fluorescence of a third liposome population containing 0.5 and 1 mol% of NBD-PE and Rh-PE respectively was taken as a control for 100% of fusion. The fluorescence emission of N-NBD-PE was monitored at 530 nm with an excitation wavelength of 460 nm. The percent of fusion was calculated according to the following equation:

$$\%\text{Fusion} = [(F_t - F_0)/(F_\infty - F_0)] \times 100 \quad (1)$$

where F_t is the fluorescence intensity at time t, F_0 is the fluorescence at time 0 and F_∞ is the final fluorescence determined with the "mock fused" vesicles.

2.7. Sequence and structure analysis

In order to detect the presence of any putative conserved sequence motif related to fusion among GAPDH, GDH, SDH and ADH the following procedure was applied. First, homologue sequences for each protein were retrieved from UniprotKB sequence database using PSI-BLAST [19]. Multiple sequence alignments were built using CLUSTALX [20], and Hidden–Markov profiles [21] were extracted using the HMMER package and compared to each other with LogoMat-P [22]. Alternatively, conserved motifs among each group were extracted using MEME System [23] and compared using LAMA software [24]. With the aim of searching any common structural motif, protein structure comparison was performed using OPAAS web server [25].

2.8. Electrostatic potentials and free energies calculations

Both, electrostatic potential and free energies were obtained from a modified version of the DelPhi program [26] that solves the nonlinear Poisson–Boltzmann equation for protein/membrane systems [27]. In the calculations described in this work, protein molecule was represented in atomic detail, mixed phosphatidylcholine:phosphatidylserine bilayers

were built as previously described [27] and the solvent is described in terms of a bulk dielectric constant. The protein molecules do not interact with each other so the binding of a single protein molecule to the surface can be analyzed. Radius and partial charge assigned to each amino acid residue were taken from a CHARMm22 parameter set [28]; those used for the lipids are the ones described by Peitzsch et al. [29]. The atomic coordinates for the biological units of ADH (2hcy), GAPDH (1j0x), GDH (1hwx) were retrieved from PDB. For SDH a model was built as described below. Protein side chains pKa calculations were performed through H++ server [30,31] in order to assign proper titration states.

The molecular models built were mapped onto a three-dimensional cubic grid of 301 points (final resolution of 2 grid/Å), each of which represents a small region of the protein, membrane, or solvent. A dielectric constant of 2 is assigned to the regions inside the molecular surfaces of the protein and membrane and 80 was used for the rest of the system [32]. An ion exclusion layer is added to the solutes and extends 2 Å beyond the molecular surfaces [27]. The nonlinear Poisson–Boltzmann equation is solved in the finite difference approximation, and the numerical calculation of the potential is iterated to convergence, which is defined as the point at which the electrostatic potential changes $<10^{-4}$ kT/e between successive iterations.

The non-specific electrostatic contribution to the binding free energy of interaction (ΔG_{el}) was calculated according to Eq. (2):

$$\Delta G_{el} = G_{e/PM} - \left[G_{e/P} + G_{e/M}\right] \quad (2)$$

where (G_{elPM}) is the electrostatic free energy of a protein–membrane complex; (G_{elP}) and (G_{elM}) are the electrostatic free energy for the protein and the membrane taken separately.

The electrostatic contribution to the free energy of binding for the protein–membrane system as a function of the protein orientation was explored. These calculations were designed to estimate the protein orientation in which it is most strongly attracted to the membrane, *i.e.*, the orientation of minimal ΔG_{el}. For peripheral association the electrostatic contribution to binding free energies is well described by considering the minimum free energy alone [27,33,34].The relative position of the protein in relation to the membrane could be defined by three Euler rotation angles (phi, psi, theta) and the distance between the molecular surfaces of the protein and the membrane as *r*. For each protein 62 different orientations were tested, fixing psi = 0, *r* = 3 Å and evaluating ΔG_{el} as a function of phi and theta. The orientation phi = 0, theta = 0 was taken as the one that has the longest axis of the molecule aligned to the *X*-axis, and the next largest to the *Y*-axis.

2.9. SDH model building

Sheep liver sorbitol dehydrogenase was modelled by comparative modelling using Modeller [35] taking human sorbitol dehydrogenase (1pl7) as template. Taking into account the high degree of identity/similarity (87%/93%) between the model and template sequences and the presence of only 3 gaps located on solvent accessible loops, the alignment was straightforward. The protein was modelled as a tetramer with 4 Zn bound atoms as the hSDH biological unit.

3. Results

3.1. Fusion, aggregation and leakage induced by NAD(P)H dehydrogenases

The ability of ADH, GAPDH, GDH and SDH to induce membrane aggregation and fusion of the DOPC:DOPS SUV system was measured using spectroscopic techniques. The criterion used for the selection of these proteins was based on the availability of structural data derived from experimental or comparative modelling.

Vesicles aggregation was measured following the light scattering at 450 nm (Fig. 1A). The addition of micromolar concentrations of GAPDH or SDH to a suspension of SUV leads to a rapid liposomal aggregation. On the contrary, GDH exhibited a latency period of nearly 40 s before aggregation starts, while ADH was incapable of inducing vesicle aggregation.

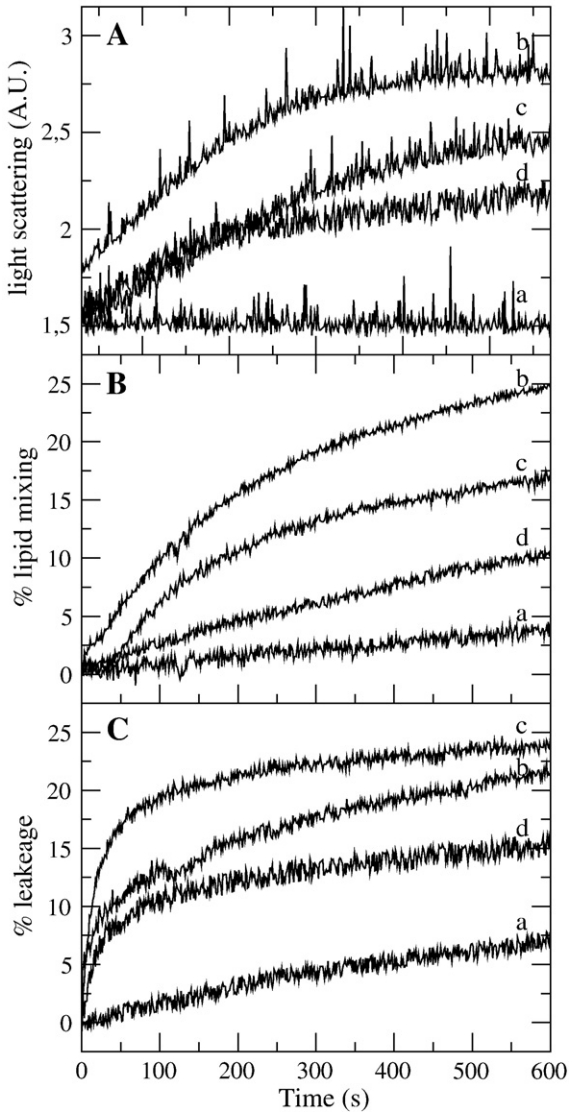

Fig. 1. Time course of aggregation (A), fusion (B) and release of content (C) upon addition of 0.1 μM ADH (a), GAPDH (b), GDH (c), SDH (d). Protein was added to DOPC:DOPS (8:1) SUV and light scattering, lipid mixing or leakage were measured. Lipid concentration was 50 μM for all assays. Experiments were triplicated.

Fig. 1B presents comparative results of the enzymes fusogenic activity, monitored with the RET assay. The data readily demonstrate that GAPDH was more efficient at inducing lipid mixing than the other dehydrogenases tested. For GAPDH it was found that the protein/lipid ratio required to induce 25% lipid mixing was 1:500. In comparison, GDH induced 17% and SDH 11% of lipid mixing respectively at the same protein/lipid ratio, while ADH fusogenic activity was hardly detectable (<3% RET). These data strongly support the idea that GAPDH, GDH and SDH were capable of inducing membranes to merge. It is important to note that fusion induced by GDH followed a kinetic similar to aggregation exhibiting the same latency period.

In order to test the capability of the proteins to alter the membrane integrity and also change its permeability, leakage of the pre-encapsulated fluorescent complex Tb/DPA from the liposomes was evaluated. A higher extent of leakage was immediately induced upon addition of GDH (25%) than for GAPDH(22%) and SDH (15%) while ADH

was able to induce the release of only the 7% of the complex Tb/DPA from the liposomes (Fig. 1C). It is important to notice that, in contrast to fusion, leakage induced by GDH and SDH reaches a plateau and no latency period is observed.

3.2. Sequence and structural analysis

It was tempting to speculate that a conserved motif implicated in the fusion ability could be present in GAPDH, GDH, and SDH, mimicking the conserved fusion peptide from viral fusion systems. To this end, the algorithm described on Materials and methods was applied, and the results showed that the unique conserved region is the nucleotide binding motif GXGXXG located within the FAD/NAD(P)-binding Rossmann fold Superfamily clan (CL0063) domain. However, no direct relationship could be found with the fusogenic ability, since this motif is also present in ADH. These results are in good agreement with experimental data in which the K_m for the substrate and for NADH in the presence and in the absence of phospholipid vesicles did not exhibit any significant difference (data not shown).

In order to search for any structural motif conserved across GAPDH, GDH and SDH which resemble the four helix bundle present in other fusion systems, a protein comparative analysis was performed using OPAAS web server. The unique structural feature common to the four proteins, corresponds to a segment within the domain annotated in CATH database as α/β class (code 3), with a 3 layer *bba* sandwich architecture (code 3.50), exhibiting a Rossmann fold topology (code 3.40.50) and within the Rossmann fold NAD(P)-binding Rossmann-like homologous superfamily (code 3.40.50.720). The fact that this structural motif is also present in ADH, is not suggestive of a relationship between this fold and the fusogenic capability.

From protein sequence and structure analysis it is not evident any common feature attributable to the fusogenic capability. In this way, a model for the protein–membrane complex is desirable since it could give some clues on the interactions among them and shed some light on the molecular basis of the membrane binding, aggregation and fusion capability of these redox enzymes.

3.3. Protein–membrane interaction studies

The molecular basis of the initial interaction between a protein and a charged surface is essentially an understanding of the role of electrostatics in intermolecular interactions [36].

Accordingly, the fusion extent induced by GAPDH, is significantly dependent on the pH and on the salt concentration of the medium [12]. GDH and SDH show the same behavior (data not shown) suggesting that the electrostatic forces could be playing an important role on the fusogenic activity of these redox proteins, and thus on the different steps involved within this process, *i.e.* membrane binding, aggregation and or destabilization.

The electrostatic contribution to the binding free energy of interaction (ΔG_{el}) was obtained as the difference between the electrostatic free energy of the protein–membrane complex and the electrostatic free energy for the protein and the membrane infinitely far apart as described in Materials and methods. To perform this evaluation, the proteins were docked at the surfaces of the membranes at different orientations in relation to the membrane plane.

The obtained ΔG_{el} as a function of the protein's Euler rotation angles is represented in a two-dimensional contour plot (Fig. 2). The central result is that GAPDH, GDH, SDH and also ADH can acquire at least one orientation in which the electrostatic contribution to the binding free energy is large enough to account, by itself, for strong membrane binding.

The protein capability to bind to lipid vesicles was experimentally tested by means of Trp intrinsic fluorescence quenching assays. The quenching parameter (K_{SV}) obtained by analyzing the Stern–Volmer plots of each enzyme in the absence and in the presence of SUV is shown in Table 1. The addition of the lipid vesicles leads to an apparent decrease in the Trp accessibility evidenced by the K_{SV} decrease, suggesting that the Trp residues in membrane bound GDH, GAPDH, SDH and also ADH are less exposed in the presence of the vesicles.

Liposome aggregation capability for each protein could also be deduced from the free energy of interaction landscape depicted on Fig. 2. Proteins should have at least two discrete regions capable of binding membranes for the vesicles aggregation process to occur. In

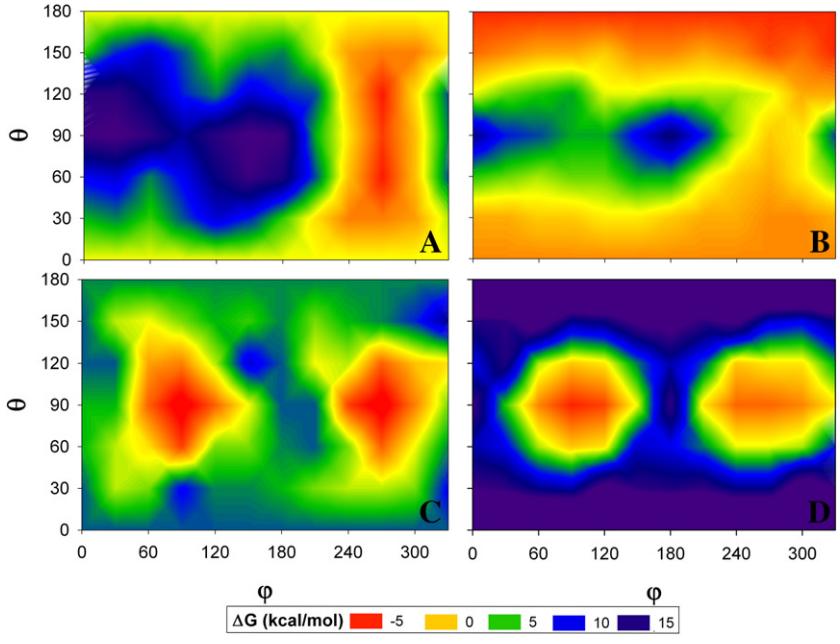

Fig. 2. Landscape representation of the ΔG_{el} of ADH (A), GAPDH (B), GDH (C) and SDH (D) at pH 7.40 bound to a 8:1 PC/PS membrane as a function of the protein's Euler rotation angles, phi and theta. For each protein 62 different orientations were tested, fixing psi=0, r=3 Å. The orientation phi=0, theta=0 is taken as that which has the longest axis of the molecule aligned to the *X*-axis, and the next largest to the *Y*-axis. ΔG_{el} was calculated according to Eq. (1).

Table 1
Trp intrinsic fluorescence quenching assays

	K_{sv} (M^{-1})	
	Without SUV	With PC:PS-SUV
ADH	0.0021± 0.0002	0.0014± 0.0001
GAPDH	0.0022± 0.0003	0.0018± 0.0002
GDH	0.0020± 0.0001	0.0015± 0.0001
SDH	0.0016± 0.0001	0.0009± 0.0001

The quenching experiments were carried out by the addition of KI on a 0.1 μM protein solution in the absence or presence of 50 μM SUVs. The slope of the Stern–Volmer plot, obtained from the quenching experiments, is the Stern–Volmer constant (K_{SV}).

Table 2
In silico alanine-scanning mutagenesis

	ΔG_{el} (kcal/mol)
ADH	−4.29
ADH_K21A	2.70
ADH_K27A	4.70
ADH_K29A	2.70
GAPDH	−5.09
GAPDH_K83A	4.90
GAPDH_K110A	5.90
GAPDH_K114A	1.91
GAPDH_K142A	1.91
GDH	−7.41
GDH_K419A	4.59
GDH_K420A	3.59
SDH	−5.09
SDH_K2A	1.90
SDH_K75A	0.91

Alanine-scanning mutagenesis was performed over all basic residues of GAPDH, GDH, SDH and ADH and the electrostatic free energy of binding for each mutant was reevaluated. Only mutations able to induce changes on ΔG_{el} larger than 2.5 kcal/mol are listed.

this way, Fig. 2 shows that GAPDH, GDH and SDH have two negative ΔG_{el} spots, while ADH exhibits only a single negative ΔG_{el} spot. This prediction is in good agreement with the results shown on Fig. 1B.

Fig. 3 shows the orientation of minimum electrostatic free energy between ADH, GAPDH, GDH or SDH and a 8:1 PC/PS bilayer along with the electrostatic potential profile at pH 7.4. The electrostatic free energy of interaction for this orientation was −4.29 kcal/mol for ADH; −5.09 kcal/mol for GAPDH; −7.41 kcal/mol for GDH and −5.09 kcal/mol for SDH.

Many proteins have a cluster of basic residues that facilitate their association to membranes containing acidic lipids [27]. In order to test this possibility and characterize the protein–membrane interaction region (hot spots), basic residues were systematically replaced by Ala (Alanine-scanning) and the binding electrostatic free energy was recalculated for each mutant. Mutations able to induce a weakening of more than 50-fold ($\Delta\Delta G_{el}$>2.5 kcal/mol) are shown in Table 2 and shaded in green in Fig. 3. It is important to notice that all of the listed residues are located in the proposed protein–membrane contact region.

As it is evident from Fig. 3, GAPDH, GDH and SDH have a main positive electrostatic potential. On the contrary, in ADH, the electropositive potential is only located in the region surrounding the membrane binding, while the remaining portion of the protein is mainly acidic. An electropositive potential which arises from a region with negative curvature in the protein surface and extends to the membrane is clear in the four enzymes. These crevices are oriented facing the membrane. Fig. 4 shows that GDH has the crevice with higher depth and length (25×10 Å) while ADH presents the smaller one (6×10 Å). These surfaces with negative curvature could be involved in the membrane destabilization once the protein–membrane complex has been formed. In fact, the extent of the aqueous content leakage is in accordance with the size of the crevices, *i.e.* GDH>GAPDH>SDH>ADH.

4. Discussion

The enzymes studied herein are well-known for their redox activity and despite the fact that they lack structural features present in viral or SNARE's fusion systems, such as the fusion peptide or the helix bundle motif, they can promote the aggregation and fusion of phospholipid vesicles. Therefore, they could represent a simple and attractive model to study the molecular mechanisms that drives membrane fusion.

Our experimental results showed that GAPDH, GDH and SDH are capable of inducing aggregation and fusion of negatively charged liposomes. The kinetics of both process suggest that they are coupled. ADH was incapable of inducing membrane aggregation and in addition no fusion was detected in the presence of this enzyme. However, ADH could induce a small perturbation in the membrane evidenced by the leakage of the aqueous content. These observations suggest that vesicle membrane permeabilization occurs independently of vesicle fusion. Reinforcing this idea, the vesicles leakage kinetic induced by GDH has a hyperbolic behavior without any latency period observed in fusion experiments.

Since bioinformatics analysis of GAPDH, GDH, SDH and ADH did not give any conserved sequence or structural motif to be related with the fusogenic activity, a model of how these proteins attach to a membrane could shed light not only on the binding process but also on membrane aggregation and destabilization. The orientation by which a protein is immobilized on a surface plays an important role in determining the extent of interaction and its consequent biological function. However, due to the size of the protein–membrane assemblies, it is difficult to obtain reliable experimental data using classical structural techniques [37]. In this way, considering that electrostatics are the driving forces of the protein–membrane complex

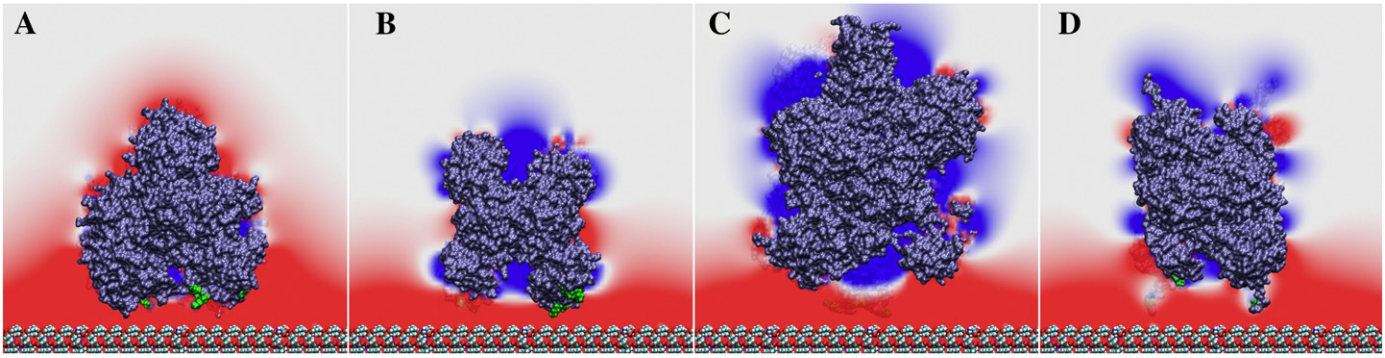

Fig. 3. Model of membrane interaction of ADH (A), GAPDH (B), GDH (C) or SDH (D) and PC/PS (8:1) bilayer in the orientation of minimum free energy. The electrostatic properties of the system in 20 mM salt solution pH 7.40 were calculated by using DelPhi software. The protein molecular surface is colored in gray and the electrostatic potential with a color-code map ranging from −1 kT/e (red) to 1 kT/e (blue) and neutral potentials are white. The color-code maps show the electrostatic potentials in a cross section through the middle plane of the molecule. Residues listed on Table 2 are shaded on green. (For interpretation of the references to color in this figure legend, the reader is referred to the web version of this article.)

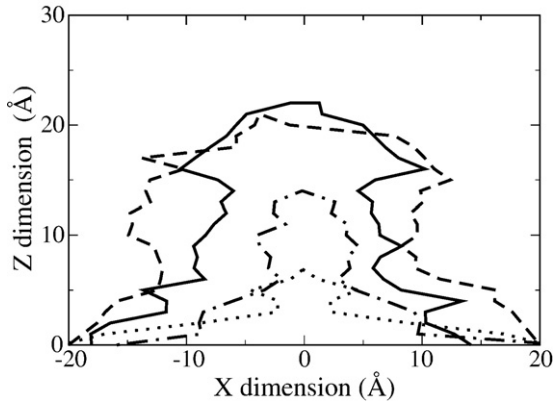

Fig. 4. Cross-section of the molecular surface through the *X*–*Z* midplane of Fig. 3 for ADH (dotted line); GAPDH (straight line); GDH (dashed line) and SDH (dash-dotted line). The molecular surfaces were calculated by using SURF from UNC-Chapel Hill [42].

assembly, a computational approach based on testing electrostatic free energy of interaction was used to predict the most probable orientation between the protein and the membrane surface.

The combination of FDPB methodology and *in silico* alanine-scanning mutagenesis allows the identification of protein–membrane interaction hot spots on the protein surface. Based on our calculations, mutations that resulted on changes on the electrostatic free energy of interaction large enough to account for at least a 50-fold decrease on binding were recognized. It is important to note that all sensitive residues are located in the predicted binding interfaces and constitutes a valuable guide for experimental mutagenesis design.

Using an immunochemical approach, Kaneda et al. [38] identified a sequence region (residues 70–94) on GAPDH involved in phosphatidylserine binding. The protein–membrane complex proposed in this work (Fig. 3B), locates these residues on the protein–membrane contact interface.

It is important to consider that many results of the present work are based on the FDPB methodology, which has been extensively tested and shown to work remarkably well in many applications involving non-specific binding. For non-specific protein/membrane interactions, the FDPB methodology predicted the ionic strength and lipid composition dependence of the membrane binding of simple basic peptides [27] and charybdotoxin [33] with deviations from experimental values on the order of 0.2 kcal/mol or less.

The FDPB methodology also allowed predicting the aggregation capability through the evaluation of the free energy of association as a function of the orientation between the protein and the membrane (Fig. 2). The presence of more than one valley on the binding free energy landscape would indicate the capability of the protein to bind to more than one vesicle. In this way, from Fig. 2 it is quite straightforward why ADH is unable to aggregate phospholipid vesicles at pH 7.4 and therefore incapable of inducing fusion at this pH.

However, the aggregation is necessary, but not sufficient for membrane fusion to occur. Once the membranes are brought together, membrane destabilization must be induced to start the lipid merging. In this way, the protein–membrane complex in its minimum ΔG_{el} obtained for GAPDH, GDH, SDH and ADH suggests the presence of concave surfaces on the protein facing the membrane. From these crevices, an electropositive potential arises towards the membrane, which might exert an attractor force over the negatively charged phospholipids present on the membrane, inducing a perturbation in the bilayer packing. In this way, the capability to induce vesicle aqueous content leakage, *i.e.* GDH>GAPDH>SDH>ADH is in accordance with the size and charge density of the protein's crevice (Figs. 4 and 1C).

The relationship between curved protein surfaces with cellular fusion via the generation of local membrane curvature was previously suggested [39]. In fact, proteins with N-BAR (Bin/amphiphysin/Rvs) domains have a concave face involved in the plastering of the negatively charged cell membrane to the positively charged concave surface. These domains are involved in various cellular processes related to membrane fusion, such as synaptic vesicle endocytosis. Moreover, membrane fusion events have been related to local changes in membrane curvature during the formation of kinetic intermediates [40,41].

In spite of membrane fusion is a complex biophysical event, the model presented herein aids to give some insights on the significance of electrostatics on the first steps of the process, *i.e.* protein–membrane binding, aggregation and destabilization. Nevertheless it should be noted that many of the conclusions are derived from a static model based on the assumption of a rigid membrane whose structure does not react to the approach of a charged molecule. Future experiments and molecular dynamics calculations shall shed light into the membrane response upon protein binding.

The physiological meaning of a possible role for some cytoplasmic dehydrogenases in membrane fusion is uncertain, but these oxidoreductases are widely spread in nature. Although the precise role of these proteins in cellular function is uncertain, they could be just an evolutionary reminiscence useful in the cell before sophisticated membrane fusion systems like SNARE appeared.

Acknowledgements

This research was supported by the Consejo Nacional de Investigaciones Científicas y Técnicas (CONICET) PIP 6399, RIB (Red Iberoamericana de Bioinformática), Secretaría de Ciencia y Técnica de la Universidad Nacional de Tucumán (CIUNT) 26/D-313, Argentina and FONCYT (PAE 22642). JDLR thanks to the Spanish Ministery of Health (MSyC) for the Project (FIS ISCiii PI061153). The authors are grateful to Dr. Max Valentinuzzi for his valuable discussions.

References

[1] S.L. Leikin, M.M. Kozlov, L.V. Chernomordik, V.S. Markin, Y.A. Chizmadzhev, Membrane fusion: overcoming of the hydration barrier and local restructuring, Journal of Theoretical Biology 129 (1987) 411–425.
[2] W. Weissenhorn, A. Hinz, Y. Gaudin, Virus membrane fusion, FEBS Letters 581 (2007) 2150–2155.
[3] M. Leabu, Membrane fusion in cells: molecular machinery and mechanisms, Journal of Cellular and Molecular Medicine 10 (2006) 423–427.
[4] T.H. Sollner, Intracellular and viral membrane fusion: a uniting mechanism, Current Opinion in Cell Biology 16 (2004) 429–435.
[5] M.K.a.A.H.J. White, Membrane fusion proteins of enveloped animal viruses, Quarterly Reviews of Biophysics 16 (1983) 151–192.
[6] W.R. Gallaher, Detection of a fusion peptide sequence in the transmembrane protein of human immunodeficiency virus, Cell 50 (1987) 327–328.
[7] E. Hunter, E. Hill, M. Hardwick, A. Bhown, D.E. Schwartz, R. Tizard, Complete sequence of the *Rous sarcoma* virus env gene: identification of structural and functional regions of its product, Journal of Virology 46 (1983) 920–936.
[8] M.A. Whitt, P. Zagouras, B. Crise, J.K. Rose, A fusion-defective mutant of the vesicular stomatitis virus glycoprotein, Journal of Virology 64 (1990) 4907–4913.
[9] W.R. Gallaher, Similar structural models of the transmembrane proteins of Ebola and avian sarcoma viruses, Cell 85 (1996) 477–478.
[10] S.G. Peisajovich, Y. Shai, Viral fusion proteins: multiple regions contribute to membrane fusion, Biochimica et Biophysica Acta 1614 (2003) 122–129.
[11] A.E. Lopez Vinals, R.N. Farias, R.D. Morero, Characterization of the fusogenic properties of glyceraldehyde-3-phosphate dehydrogenase: fusion of phospholipid vesicles, Biochemical and Biophysical Research Communications 143 (1987) 403–409.
[12] R.D. Morero, A.L. Vinals, B. Bloj, R.N. Farias, Fusion of phospholipid vesicles induced by muscle glyceraldehyde-3-phosphate dehydrogenase in the absence of calcium, Biochemistry 24 (1985) 1904–1909.
[13] M.A. Sirover, New insights into an old protein: the functional diversity of mammalian glyceraldehyde-3-phosphate dehydrogenase, Biochimica et Biophysica Acta 1432 (1999) 159–184.
[14] E.G. Finer, A.G. Flook, H. Hauser, Mechanism of sonication of aqueous egg yolk lecithin dispersions and nature of the resultant particles, Biochimica et Biophysica Acta 260 (1972) 49–58.
[15] E.A. Burstein, N.S. Vedenkina, M.N. Ivkova, Fluorescence and the location of tryptophan residues in protein molecules, Photochemistry and Photobiology 18 (1973) 263–279.
[16] S.S. Lehrer, Solute perturbation of protein fluorescence. The quenching of the tryptophyl fluorescence of model compounds and of lysozyme by iodide ion, Biochemistry 10 (1971) 3254–3263.
[17] J. Wilschut, N. Duzgunes, R. Fraley, D. Papahadjopoulos, Studies on the mechanism of membrane fusion: kinetics of calcium ion induced fusion of phosphatidylserine

vesicles followed by a new assay for mixing of aqueous vesicle contents, Biochemistry 19 (1980) 6011–6021.
[18] D.K. Struck, D. Hoekstra, R.E. Pagano, Use of resonance energy transfer to monitor membrane fusion, Biochemistry 20 (1981) 4093–4099.
[19] S.F. Altschul, T.L. Madden, A.A. Schaffer, J. Zhang, Z. Zhang, W. Miller, D.J. Lipman, Gapped BLAST and PSI-BLAST: a new generation of protein database search programs, Nucleic Acids Research 25 (1997) 3389–3402.
[20] J.D. Thompson, T.J. Gibson, F. Plewniak, F. Jeanmougin, D.G. Higgins, The CLUSTAL_X windows interface: flexible strategies for multiple sequence alignment aided by quality analysis tools, Nucleic Acids Research 25 (1997) 4876–4882.
[21] S.R. Eddy, Profile hidden Markov models, Bioinformatics 14 (1998) 755–763.
[22] B. Schuster-Bockler, A. Bateman, Visualizing profile–profile alignment: pairwise HMM logos, Bioinformatics 21 (2005) 2912–2913.
[23] T.L. Bailey, N. Williams, C. Misleh, W.W. Li, MEME: discovering and analyzing DNA and protein sequence motifs, Nucleic Acids Research 34 (2006) W369–373.
[24] S. Pietrokovski, Searching databases of conserved sequence regions by aligning protein multiple-alignments, Nucleic Acids Research 24 (1996) 3836–3845.
[25] E.S. Shih, R.C. Gan, M.J. Hwang, OPAAS: a web server for optimal, permuted, and other alternative alignments of protein structures, Nucleic Acids Research 34 (2006) W95–98.
[26] K. Gallagher, K. Sharp, Electrostatic contributions to heat capacity changes of DNA–ligand binding, Biophysical Journal 75 (1998) 769–776.
[27] N. Ben-Tal, B. Honig, R.M. Peitzsch, G. Denisov, S. McLaughlin, Binding of small basic peptides to membranes containing acidic lipids: theoretical models and experimental results, Biophysical Journal 71 (1996) 561–575.
[28] B. Brooks, R. Bruccoleri, B. Olafson, D. States, S. Swaminathan, M. Karplus, CHARMM: a program for macromolecular energy, minimization, and dynamics calculations, Journal of Computational Chemistry 4 (1983) 187–217.
[29] R.M. Peitzsch, M. Eisenberg, K.A. Sharp, S. McLaughlin, Calculations of the electrostatic potential adjacent to model phospholipid bilayers, Biophysical Journal 68 (1995) 729–738.
[30] J.C. Gordon, J.B. Myers, T. Folta, V. Shoja, L.S. Heath, A. Onufriev, H++: a server for estimating pKas and adding missing hydrogens to macromolecules, Nucleic Acids Research 33 (2005) W368–W371.
[31] D. Bashford, M. Karplus, pKa's of ionizable groups in proteins: atomic detail from a continuum electrostatic model, Biochemistry 29 (1990) 10219–10225.
[32] K.A. Sharp, B. Honig, Electrostatic interactions in macromolecules: theory and applications, Annual Review of Biophysics and Biophysical Chemistry 19 (1990) 301–332.
[33] N. Ben-Tal, B. Honig, C. Miller, S. McLaughlin, Electrostatic binding of proteins to membranes. Theoretical predictions and experimental results with charybdotoxin and phospholipid vesicles, Biophysical Journal 73 (1997) 1717–1727.
[34] A. Arbuzova, L. Wang, J. Wang, G. Hangyas-Mihalyne, D. Murray, B. Honig, S. McLaughlin, Membrane binding of peptides containing both basic and aromatic residues. Experimental studies with peptides corresponding to the scaffolding region of caveolin and the effector region of MARCKS, Biochemistry 39 (2000) 10330–10339.
[35] A. Sali, T.L. Blundell, Comparative protein modelling by satisfaction of spatial restraints, Journal of Molecular Biology 234 (1993) 779–815.
[36] M.T. Neves-Petersen, S.B. Petersen, Protein electrostatics: a review of the equations and methods used to model electrostatic equations in biomolecules—applications in biotechnology, Biotechnology Annual Review 9 (2003) 315–395.
[37] A.H. Talasaz, M. Nemat-Gorgani, Y. Liu, P. Stahl, R.W. Dutton, M. Ronaghi, R.W. Davis, Prediction of protein orientation upon immobilization on biological and nonbiological surfaces, Proceedings of the National Academy of Sciences of the United States of America 103 (2006) 14773–14778.
[38] M. Kaneda, K. Takeuchi, K. Inoue, M. Umeda, Localization of the phosphatidylserine-binding site of glyceraldehyde-3-phosphate dehydrogenase responsible for membrane fusion, Journal of Biochemistry (Tokyo) 122 (1997) 1233–1240.
[39] P.D. Blood, G.A. Voth, Direct observation of Bin/amphiphysin/Rvs (BAR) domain-induced membrane curvature by means of molecular dynamics simulations, Proceedings of the National Academy of Sciences of the United States of America 103 (2006) 15068–15072.
[40] D.P. Siegel, Energetics of intermediates in membrane fusion: comparison of stalk and inverted micellar intermediate mechanisms, Biophysical Journal 65 (1993) 2124–2140.
[41] F.M. Goni, H. Ostolaza, *E. coli* alpha-hemolysin: a membrane-active protein toxin, Brazilian Journal of Medical and Biological Research 31 (1998) 1019–1034.
[42] F.P.B.A. Varshney, W.V. Wright, Linearly scalable computation of smooth molecular surfaces, IEEE Computer Graphics and Applications 14 (1994) 19–25.